COMPUTATIONAL AND STRUCTURAL BIOTECHNOLOGY JOURNAL

Review

Illuminating amyloid fibrils: Fluorescence-based single-molecule approaches

Lauren J. Rice [a,b], Heath Ecroyd [a,b,*], Antoine M. van Oijen [a,b,*]

[a] Molecular Horizons and School of Chemistry and Molecular Bioscience, University of Wollongong, Wollongong, NSW 2522, Australia
[b] Illawarra Health & Medical Research Institute, Wollongong, NSW 2522, Australia

A B S T R A C T

The aggregation of proteins into insoluble filamentous amyloid fibrils is a pathological hallmark of neurodegenerative diseases that include Parkinson's disease and Alzheimer's disease. Since the identification of amyloid fibrils and their association with disease, there has been much work to describe the process by which fibrils form and interact with other proteins. However, due to the dynamic nature of fibril formation and the transient and heterogeneous nature of the intermediates produced, it can be challenging to examine these processes using techniques that rely on traditional ensemble-based measurements. Single-molecule approaches overcome these limitations as rare and short-lived species within a population can be individually studied. Fluorescence-based single-molecule methods have proven to be particularly useful for the study of amyloid fibril formation. In this review, we discuss the use of different experimental single-molecule fluorescence microscopy approaches to study amyloid fibrils and their interaction with other proteins, in particular molecular chaperones. We highlight the mechanistic insights these single-molecule techniques have already provided in our understanding of how fibrils form, and comment on their potential future use in studying amyloid fibrils and their intermediates.

© 2021 The Author(s). Published by Elsevier B.V. on behalf of Research Network of Computational and Structural Biotechnology. This is an open access article under the CC BY-NC-ND license (http://creativecommons.org/licenses/by-nc-nd/4.0/).

Contents

* Corresponding authors at: Molecular Horizons and School of Chemistry and Molecular Bioscience, University of Wollongong, Wollongong, NSW 2522, Australia.
  E-mail addresses: heathe@uow.edu.au (H. Ecroyd), vanoijen@uow.edu.au (A.M. van Oijen).

1. Introduction

Most proteins must fold into a specific 3D conformation in order to achieve (and maintain) their functional and active state [1]. During the folding process the polypeptide chain typically samples numerous conformations until the most energetically favourable fold is reached [1,2]. Under conditions of cellular stress (*e.g.* changes in pH or temperature) or as a result of genetic mutations, proteins may not fold correctly or become misfolded, resulting in hydrophobic regions normally buried within the interior of the protein becoming exposed on the surface [3,4]. Misfolded proteins can be refolded or discarded by cellular protein-quality control mechanisms that include molecular chaperones [5,6] and degradation pathways (such as the ubiquitin proteasome pathway and autophagy).

If protein-quality control mechanisms are (or become) ineffective, misfolded proteins can self-associate to form amorphous or fibrillar aggregates [3]. Fibrillar protein aggregates, in the form of highly ordered, β-sheet rich 'amyloid' fibrils, have received much attention due to their association with various diseases, including neurodegenerative disorders such as Alzheimer's Disease (AD), Parkinson's disease (PD), and Amyotrophic Lateral Sclerosis [3,7–9]. These fibrillar protein aggregates and the mechanism by which they form are the focus of this review. Although the presence of amyloid fibrils within insoluble, proteinaceous inclusions has been widely documented [10,11], mechanistic details regarding how fibrils form and cause harm to cells remain to be elucidated. This is due, at least in part, to the complex and heterogeneous nature of the fibril-forming process and the oligomeric state of the aggregated protein.

Many of the assays traditionally employed to measure amyloid fibril formation utilise bulk biochemical techniques, which are based on the ensemble-averaging of a large number of molecules in solution. These assays typically report on β-sheet formation (indicative of fibril formation) and any ensemble-averaged changes to this process due to manipulation of the surrounding environment. Single-molecule techniques are valuable methods to study the heterogenous biological process of fibril formation as they can unmask mechanistic details "hidden" by ensemble-based measurements [12,13]. Single-molecule techniques comprise an array of powerful methods that include cryo-electron microscopy, optical tweezers, mass photometry [14] and fluorescence-microscopy approaches [13,15]. Single-molecule fluorescence-microscopy techniques can provide mechanistic detail about molecular interactions such as enzymatic turnover rates, dissociation and association rates, and stoichiometries of interacting species [16–18]. As such, they are considered 'bottom-up' methods in that by visualising and analysing information from single molecules, they allow information about an entire system to be ascertained. Such approaches can be particularly powerful when applied to biological processes that depend on rare or transient intermediate species/states in order to proceed. One such process is the formation of amyloid fibrils, wherein these species are often masked by ensemble-averaging methods. This review focusses on the use of fluorescence-based single-molecule techniques to study amyloid fibrils: their formation, disaggregation, and the interactions that govern these processes.

We first compare how Total Internal Reflection Fluorescence (TIRF) and confocal microscopy can be utilised as single-molecule fluorescence methods, before outlining the techniques of stepwise photobleaching analysis, Förster Resonance Energy Transfer (FRET), two-colour coincident detection (TCCD) and fluorescence correlation spectroscopy (FCS). We review how each of these methods have been used to study amyloid fibril formation at the single-molecule level, and highlight their future potential in understanding the molecular mechanisms that drive this process. We conclude by discussing single-molecule techniques that have been employed to investigate how molecular chaperones interact with amyloid fibrils to inhibit their formation and facilitate their disaggregation.

2. Oligomerisation and kinetics of fibril formation

The formation of amyloid fibrils occurs via a nucleation-dependent pathway in which partially folded intermediate states of proteins self-associate as a result of surface-exposed hydrophobic regions. Initiation of amyloid fibril formation and structural polymorphisms within fibrils can be triggered by factors such as genetic mutations, intracellular protein concentration, specific proteolytic cleavage and ligand binding [19]. The self-association of misfolded amyloid-precursor proteins promotes β-sheet stacking which stabilises core amyloid fibril structures [20]. This stability is facilitated by backbone hydrogen bonding between β-sheet strands of self-associated protein monomers [20], hydrogen bonding between the loops connecting β-sheets, interactions between polar and charged side chains, and interlocked β-sheets forming 'dry' steric zippers [21–23]. The ability of dyes such as Thioflavin T (ThT) to bind β-sheet structures [24,25] facilitates the study of amyloid fibrils by bulk biochemical assays and some single-molecule fluorescence techniques. These dyes typically become fluorescent once bound to β-sheet structures present in amyloid fibrils [128] and using these dyes to monitor the fibril-formation process reveals the presence of a lag phase, elongation phase, and plateau (indicating equilibrium) in the reaction [26] (Fig. 1). The lag phase is the rate-limiting step of the reaction and represents the time taken for β-sheet rich oligomers to form a sufficient percentage of nuclei or 'seeds' [27]. During the lag phase, monomeric and early-stage oligomeric species are dominant in solution, resulting in low, mostly undetectable levels of fluorescence emitted by amyloid dyes [28,29]. The association of monomers with these nuclei results in their extension and the characteristic increase in fluorescence observed during the elongation phase. The plateau phase represents the stage of the reaction when an equilibrium has been reached between all species in solution [30] (Fig. 1).

Amyloid fibrils can consist of up to six pre-fibrillar filaments, called protofibrils, which intertwine to form more rigid, straight (mature) fibrils 5–20 nm in width [31–33]. Whilst fibrils typically share a common underlying β-sheet rich architecture (initiated by oligomer formation during nucleation), there have been multiple polymorphisms of mature amyloid fibrils formed by the same protein detected by cryo-electron microscopy (EM), x-ray crystallography, and nuclear magnetic resonance (NMR), including ribbons, sheets and multi-strand cables [34]. It has been suggested that the heterogeneity of fibril and oligomer structures is related to peptide-peptide interactions that mediate formation of β-sheet twists [35]. Recently, cryo-EM technology has resulted in an increase in structural detail surrounding amyloid fibril polymorphisms. The complexity and heterogeneity of amyloid fibrils has been reviewed elsewhere [21,36] and so are only briefly discussed here.

AD [37] and PD [38] are associated with amyloid fibrils formed by the proteins Amyloid β (Aβ) and α-synuclein (α-syn), respectively. It has been found that in both cases, fibrils form by the interaction of two protofibrils via a common dimer-interface, a feature that has prompted further research into their structural characteristics [37,38]. Structural elucidation of α-syn fibrils has shown a characteristic left-handed twist morphology, extensive Greek-key topology, and that most of the residues corresponding to the genetic mutations responsible for early onset PD (*i.e.* the point
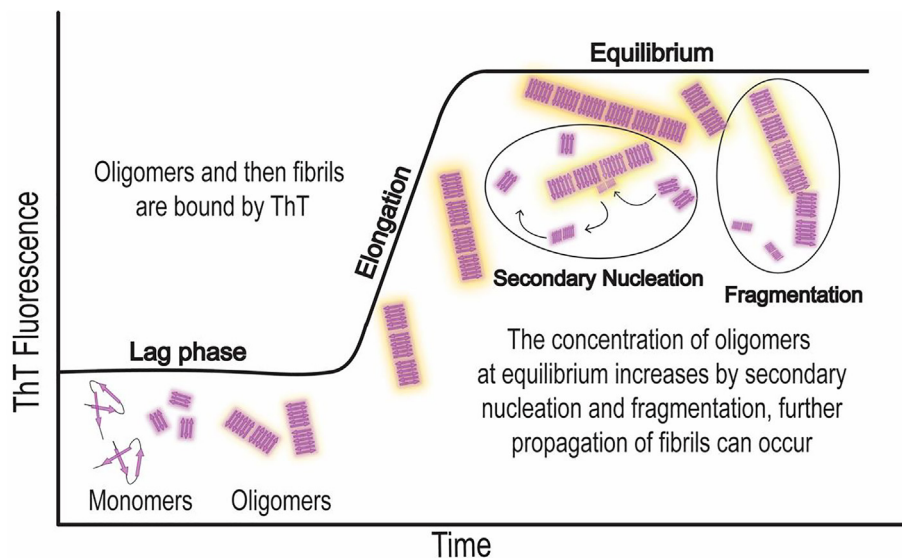
Fig. 1. The formation of amyloid fibrils as monitored by ThT fluorescence. This schematic describes the formation of amyloid fibrils from monomeric protein subunits. The lag phase represents the association between β-sheet rich monomers to form oligomers and is the rate-limiting step in the process. Production of oligomeric seeds is followed by the elongation phase during which fluorescence increases due to the rapid addition of monomers to oligomers. When an equilibrium is reached the fluorescence plateaus. Mature amyloid fibrils can facilitate secondary nucleation on their surface or undergo fragmentation. Both events generate oligomers that can further propagate fibril formation.

mutations A53T [9], E46K [39] H50Q, and G51D [40]) are located in the protofilament dimer interface or involved in protofilament stabilisation [38]. Brain-derived Aβ amyloid fibrils have a right-handed supertwist morphology [41], and thus have a major structural difference from the left-handed twist formed by *in-vitro* formed α-syn and Aβ fibrils. The array of fibril morphologies highlights the inherent heterogeneity of amyloid fibrils and the value in developing and utilising single-molecule techniques to study them.

The oligomeric intermediates formed during the process of fibril formation have received considerable attention as these are considered to be the most cytotoxic species [42–45]. These oligomers are heterogeneous, both in terms of their structure and propensity to mature into fibrils [45,46]. The formation of oligomers can occur via primary nucleation as a result of the assembly of monomers through β-sheet interactions [47] and can then act as 'seeds' for the formation of protofibrils and fibrils. Toxic oligomers can also form through processes of 'secondary nucleation' and fragmentation of mature fibrils. Secondary nucleation is catalysed by the surface of pre-existing fibrils [48–52]. The properties of the 'parent' fibril that facilitate secondary nucleation remain to be established; however, it has been postulated that hydrophobic patches on the fibril surface [53], and the ability of misfolded monomers to 'recognize' similar structures within the 'parent' fibril play a role in this process [54]. It was recently shown that decreasing the surface hydrophobicity of fibrils formed by the AD-associated Aβ(1-42) via serine substitution of hydrophobic residues exposed on the fibril surface, does not change the rate of secondary nucleation [53]. However, both α-syn [55] and Aβ(1-42) [53] are able to 'template' secondary nuclei via the exposed surface residues of the mature fibrils, wherein monomers transiently bind and form oligomers with identical morphologies to those of the templating fibril. These results suggest that structural features of fibrils, as well as the solution conditions under which they are formed [55], facilitate secondary nucleation and thus increased toxicity [54,56].

The fragmentation of mature fibrils also results in the formation of cytotoxic oligomers [51,57–60]; this is a length-dependent process whereby the stability (per monomeric unit) of fibrils decreases with increasing length and thus promotes their fragmentation into shorter oligomeric units [61]. Thus, fragmentation increases the concentration of prion-like 'seeds' in solution, in turn promoting

rapid fibril formation and the spread of toxic oligomers between tissues [59,60,62]. Furthermore, fragmentation has been implicated in the prion-like behaviour of amyloid oligomers in disease, as demonstrated by both experimental [60,63], and theoretical [59,60,62] investigations. Both secondary nucleation and fragmentation are widely acknowledged as significant contributors to the exponential phase of amyloid fibril formation [52,57,59,64,65]; however, due to the difficulty in characterising such dynamic processes using ensemble-based techniques, these processes have not yet been directly observed or fully characterised.

Amyloid fibril formation can be reversed through the process of disaggregation, wherein fibrils return to a soluble state via the release of monomers and oligomers back into solution. The disaggregation of amyloid fibrils often involves molecular chaperones, their co-chaperones, and essential nucleotide exchange factors (NEF). The most widely studied fibril disaggregation system is the Hsp70 'disaggregase', which involves a combination of Hsp70, Hsp40, and Hsp110 (a NEF) proteins [66,67]. This chaperone system is able to interact with mature amyloid fibrils, driving their disassembly back into a soluble state [68–70]. As such, the Hsp70 disaggregase has attracted interest as an avenue to combat neurodegenerative disease by potentially reversing the aggregation process [66,71–75].

3. Single-molecule techniques

Despite the advances that have been made toward understanding amyloid fibrils there are still gaps in our knowledge, especially when it comes to the mechanisms responsible for the complex processes of secondary nucleation, fragmentation, and disaggregation. Largely this gap in knowledge is attributable to the complexity of studying such heterogeneous species with ensemble-based biochemical techniques. Single-molecule methods have great potential for studying individual amyloid fibrils, and fluorescence-based single-molecule approaches have the capacity to reveal the mechanistic details that underpin the dynamic processes of secondary nucleation and fragmentation [76–79]. For example, the single-molecule technique of electron microscopy [41,80] has been instrumental in describing the structural features of amyloid fibrils including the many polymorphisms between protofibrils, mature
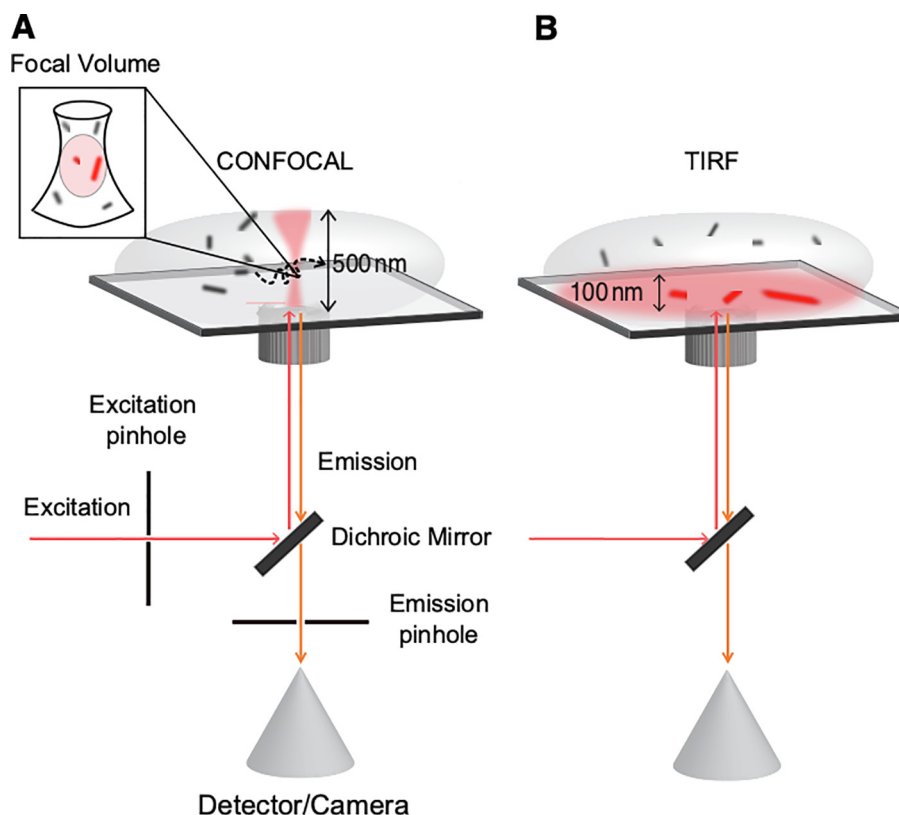
Fig. 2. Setup and comparison of fluorescence-based single-molecule microscopy techniques. (A) The schematic shows the principal components required for confocal microscopy. An excitation laser is directed through a series of mirrors, confocally aligned pinholes, and an objective lens onto a small area of the sample up to a depth of ~ 500 nm. Photons emitted from the excited samples that pass through the focal volume are detected by photon detector arrays for analysis. (B) For TIRF, the laser light is directed at the surface of a coverslip, where total internal reflection occurs by an evanescent wave, allowing emission of light from fluorophores within ~ 100 nm from the coverslip-solution interface.

fibrils, and oligomers [81,82]. Structural variations that have implications for *in vitro* research in this field have been determined by electron microscopy, with a notable example being the aforementioned differences between brain-derived and *in vitro* amyloid fibrils [41,83]. However, structural-based single-molecule techniques are limited in their ability to capture the dynamic nature of the fibril-forming process.

Fluorescence-based single-molecule techniques, wherein fluorescent moieties are attached or associate with proteins so that they can be observed, enable dynamic processes to be captured and analysed. For example, single-molecule fluorescence methods have been used successfully to describe the three-state folding process of a single protein molecule [84], fluctuating enzymatic reaction rates of single cholesterol oxidases [85], and the multiple intermediate states present in the lag phase of amyloid formation [86]. Fluorescence-based single-molecule techniques involve using optical methods to monitor fluorescence probes conjugated to biological molecules, such as proteins [87]. This includes the use of dyes that become fluorescent upon association with the structures of amyloid fibrils [88,89], and small fluorescent tags (fluorophores) that can be covalently linked to proteins. Fluorescence from these probes can be monitored at low (pico- or nano-molar) concentrations in solution using confocal microscopy, or immobilised on a surface in TIRF-based imaging (Fig. 2). It is well established that protein aggregation can be dependent on protein concentration, both *in vitro* [90,91] and *in vivo* [91]. Monitoring protein aggregation often requires the use of relatively high (micro-molar) concentrations of protein in order to study the mechanisms of aggregation on experimentally accessible timescales. However, the relatively high concentrations of protein required potentially limits the real-time study of protein aggregation by single-molecule fluores-

cence methods since these approaches typically require very low concentrations of the molecule of interest (in order to reduce background fluorescence originating from the excited volume). Thus, kinetic studies of amyloid fibril growth by single-molecule fluorescence microscopy typically require samples to be aggregated at higher concentrations and then diluted (to pico- or nano-molar concentrations – chemical crosslinking agents can be used to stabilise interactions during this process) for visualisation.

3.1. Solution-based versus surface-immobilised fluorescence single-molecule approaches

Depending on the questions asked and experimental design constraints, two different fluorescence-based approaches are typically employed to study the dynamics of biomolecules at the single-molecule level: confocal methods that detect fluorescent species freely diffusing through solution and transiently passing through a tightly-focused excitation volume, or TIRF-based techniques that monitor through time a fluorescent species that is held stationary by immobilisation to a surface (Fig. 2).

Confocal microscopy enables the visualisation of fluorescently labelled biomolecules by the creation of a diffraction-limited excitation volume inside a sample using light of a wavelength that coincides with the excitation maximum of the fluorophore to be monitored [92,93] (Fig. 2A). This excitation light is passed through confocally aligned pinholes, which results in a small volume (200 nm × 200 nm × 500 nm in dimension) being illuminated, and the emission light from that volume being detected while excluding out-of-focus sources of signal [93,94]. The traditional approach to confocal microscopy utilises 'optical sectioning', whereby the laser is scanned through a sample in all three spatial dimensions (depths

of up to 500 nm can typically be achieved), and a three-dimensional image of the sample (such as a cell) is obtained [95,96].

An alternative use of a confocal microscope is to place the confocal volume inside an aqueous solution, detecting the transient bursts of fluorescence originating from individual labelled species as they diffuse through the excitation volume [97]. Following excitation of a fluorophore, photons emitted from the molecule can be detected (typically using single-photon detector arrays), thus providing single-molecule sensitivity [96,98]. In contrast to TIRF microscopy (Fig. 2B) (discussed below), the ability to place the confocal volume deep inside a three-dimensional sample allows for molecules well above the solid–liquid interface to be visualised [99]. Subsequently, this type of confocal microscopy avoids having to immobilise molecules to a coverslip surface and thus avoids problems with steric hindrance that can arise with the TIRF microscopy approach. Single-molecule confocal microscopy enables information to be obtained on freely diffusing, fluorescently labelled molecules. Common methods that employ this approach include (i) fluorescence correlation spectroscopy (FCS), in which the apparent sizes of molecules as they pass through the confocal volume are calculated by analysis of their diffusion, and (ii) two-colour coincidence detection (TCCD), in which the simultaneous detection of two fluorescent signals within the confocal volume is used to detect biomolecular associations. Experiments that couple confocal microscopy with time-resolved single-photon detection enable the collection of data on fluorescence lifetimes [96], and fast dynamics via Förster resonance energy transfer (FRET) based applications [96,100,101] vastly increase the information that can be obtained from single-molecule confocal imaging approaches. A limitation of confocal microscopy is the size of the confocal volume: molecules can only be monitored for the period of time they remain in the confocal volume (often data acquisition has to occur on the nano- to milli-second time scales) [102].

Monitoring of single-molecule dynamics over extended time scales can be achieved using a TIRF microscopy approach (Fig. 2B). This technique involves directing the laser used for excitation of the fluorophore onto a liquid–solid interface (such as a quartz coverslip) at an angle such that the light is internally reflected. This produces an evanescent wave within the solvent at the liquid–solid interface (between the coverslip and the sample-containing aqueous solvent on its surface) [99,103]. The evanescent electro-magnetic field (created by laser excitation) decays exponentially in intensity and thus is confined to close proximity to the surface (~100 nm) (Fig. 2B). This allows selective excitation of molecules on the surface while effectively suppressing background fluorescence from other molecules in solution [103,104]. In this way TIRF can provide accurate, detailed information regarding molecular interactions [105]. Fluorescence-based TIRF methods, such as FRET (including single-molecule FRET) and photobleaching (to determine stoichiometries of interactions via the stepwise photobleaching of fluorophores) can be exploited to determine the molecular details of protein–protein interactions. Moreover, the use of fluorescent probes, such as aggregation-induced emission (AIE) dyes, in combination with TIRF-based single-molecule approaches has facilitated the visualisation and tracking of protein aggregates without the need for a fluorophore conjugated to the protein of interest [106–108].

3.2. Fluorescent probes

3.2.1. Aggregation-induced emission (AIE) dyes

Aggregation-induced emission has been demonstrated to be advantageous for the visualisation of amyloid fibrils by TIRF microscopy (Fig. 3A) [24,88,109]. Single-molecule techniques based on non-covalent interactions between the probe and protein target avoid issues that can occur when fluorescent proteins are
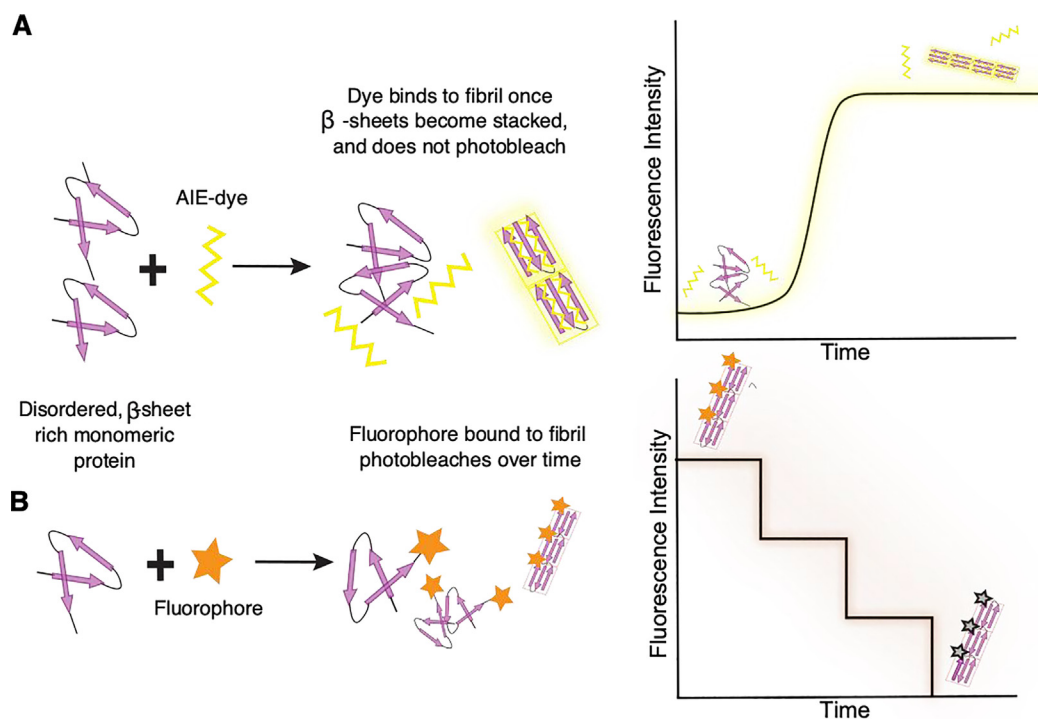
Fig. 3. Fluorescence-based approaches for monitoring amyloid fibril formation of proteins. (A) AIE dyes bind to stacked β-sheet structures within proteins, facilitating the detection of amyloid fibril formation. The signal from an AIE dye increases with β-sheet structure and is therefore used as an indicator of amyloid fibril formation. Fluorescence from AIE dyes does not photo-bleach as free dye molecules exchange with those bound to the fibril, maintaining the signal over time. (B) Fluorophores that emit light at various wavelengths can be directly conjugated to individual protein subunits, such as monomers, that make up amyloidogenic oligomers and fibrils. Photobleaching of each covalently attached fluorophore can be used to determine the number of subunits in a protein complex or fibril. In each case, emission from the fluorophore through time can be monitored by confocal or TIRF microscopy.

chemically modified for fluorescent labelling (Fig. 3B). This is particularly relevant to studies of the aggregation of α-syn as it has been reported that the fibril length and morphology can vary when the protein is tagged with fluorescent proteins or fluorophores [110]. Moreover, covalent labelling of proteins with a fluorophore can be problematic due to photobleaching that occurs during imaging. This bleaching restricts the time available for imaging and limits the timeframe for kinetic studies due to the decrease in signal intensity [111].

Fluorescent dyes including Nile Red [112] and ThT [113,114], have been used to image amyloid fibrils in TIRF studies as their non-covalent, transient interaction avoids issues with photobleaching yet still allow direct observation of protein aggregates (Fig. 3). This sustained fluorescence is facilitated by the constant exchange of dye molecules between those in solution and those bound to the amyloid structures, minimising any loss of signal over time. For example, Nile Red allows observation of exposed hydrophobic regions [115,116], as the presence of highly polar regions on proteins or lipids stimulates structural changes in the dye [117]. Specifically, changes in polarity result in altered stability of the dipole moment created by twisted intramolecular charge transfer between the donor and acceptor regions of the dye [118]. Consequently, a shift in emission wavelength [115] is observed. This phenomenon has been exploited by tracking the shift in emission wavelength of Nile Red bound to the surface of α-syn amyloid fibrils, allowing surface hydrophobicity of the fibrils to be mapped and thus the surface characteristics of the pathological protein aggregates to be determined [112,119].

The AIE properties of ThT have resulted in its application for the visualisation of amyloid fibrils [24,25,112–114,120]. An important parameter in describing the ability of a molecule to emit fluorescence is the quantum yield, defined as the ratio of photons emitted to those absorbed and reported as a number between zero and one. When free in solution, ThT molecules display rotation around a single C—C bond, resulting in a non-fluorescent 'dark' conformation, and a quantum yield approaching zero [121]. The binding of ThT to stacked β-sheets in amyloid fibrils restricts this rotation such that the absorbed light is emitted, thus increasing the quantum yield to ∼ 0.44 [24,25,121–124]. The fluorescence of ThT is relatively sensitive to the presence of amyloid fibrils due to its propensity to intercalate within β-sheet structures that are not present until oligomeric seeds and/or fibrils have formed; thus, for most proteins a fluorescent signal is not detected when the primary species in solution are monomers [24]. However, ThT has limitations with regards to using it as a fluorescent probe for single-molecule studies of protein aggregation. The relatively small Stokes shift of ThT (the emission photon wavelength is close to the wavelength of the excitation photon [125]), can cause problems in separating the emission signal from scattered excitation light [126,127]. Recently, AIE dyes with larger Stokes shifts that can be used to visualise fibrils have been described [29,108]. Apart from the advantage of an increased affinity for amyloid fibrils, another advantage of some of these recently described AIE dyes is that two-colour experiments can be performed using only one excitation laser. In these experiments, amyloid fibrils labelled with one such AIE dye, and a protein labelled with a fluorophore of a spectrally separate emission wavelength (but the same excitation wavelength) would be present. This experimental scenario would thus only require one excitation laser, whilst still being able to identify both labelled species in the sample via their different emission wavelengths. As an example, the AIE dye α-cyanostilbene derivative ASCP [29] has a very large Stokes shift (145 nm) and can be excited using a 488 nm laser light source which is commonly found in commercial fluorescence microscopes (excitation maximum at 460 nm and emission maximum at 605 nm). Recently, ASCP was used to simultaneously image molec-

ular chaperones (labelled with an AlexaFluor488 fluorophore and emission monitored at 500–550 nm) as they interacted with α-syn fibrils (excited with the 488 nm excitation wavelength and emission monitored at 675 nm and beyond) [108].

3.2.2. Conjugation of fluorophores to proteins

Fluorophores that covalently label proteins (Fig. 3B) are ideally small, bright, stable, and do not interfere with the protein structure or function. Generally, labelling of protein monomers with a small-molecule fluorophore gives the researcher flexibility with regards to the location and type of tag (optimised methods on this approach are reviewed in depth elsewhere, *e.g.* [128]). However, it is important to note that it is not always possible to attach a fluorophore to a protein without modifying its structure or function. As an example, covalent attachment of fluorophores to Aβ(1-42) has been shown to alter both the molecular weight of oligomers and the structure of mature fibrils formed by the protein, depending on the hydrophobicity and pH dependence of the fluorophore used [129].

Whilst the small oligomeric species formed early during amyloid assembly are considered to be the most pathogenic [130], they have been technically challenging to investigate using AIE dyes and bulk-ensemble approaches. This is because these oligomers are often transient and without extended β-sheet content and thus the overall fluorescent signal from these dyes in solution is very low. Studies looking to characterise these small oligomers using single-molecule fluorescence methods have typically exploited fluorophores covalently attached to the protein of interest. Using such an approach, the size of oligomeric Aβ(1-42) species was determined using TIRF microscopy and stepwise photobleaching of the attached fluorophore [131](described in more detail in Section 3.3.1). This enabled the size of Aβ(1-42) oligomers to be ascertained, and comparisons drawn between those formed in the absence and presence of putative inhibitors of fibril formation. A similar approach has been used to monitor the disaggregation of amyloid fibrils into smaller subunits (including monomers) [132–134]. Single-photon detection on a confocal microscope has been exploited to monitor the inhibition of oligomerisation and the disaggregation of pre-formed α-syn fibrils in which individual α-syn monomers were labelled with AlexaFluor-488 fluorophores [133]. By monitoring the changes in fluorescence of α-syn, this approach enabled the screening of a range of polyphenol compounds for their capacity to disaggregate the α-syn fibrils [133,134]. The mechanistic insights these single-molecule experiments provide cannot be obtained through ensemble-averaging approaches alone, thus highlighting the crucial importance of single-molecule methods in identifying regulators of fibril formation.

3.3. Fluorescence-based single-molecule techniques to study amyloid fibril formation

Single-molecule fluorescence approaches such as photobleaching, TCCD, FCS, and FRET are commonly used to investigate protein aggregation by monitoring the emission of fluorophores bound to the protein of interest (Fig. 4). These powerful techniques are capable of probing dynamics and interactions of the proteins to which they are bound.

3.3.1. Photobleaching

Photobleaching is a photophysical phenomenon wherein fluorophores undergo permanent chemical damage caused by prolonged excitation, often due to oxidation by free radicals within the imaging solution; as a result of this damage the fluorophore no longer produces a fluorescent signal (Fig. 3B) [135–138]. In the context of investigating fluorescently labelled proteins, photobleaching can be a limitation as it restricts the time available for
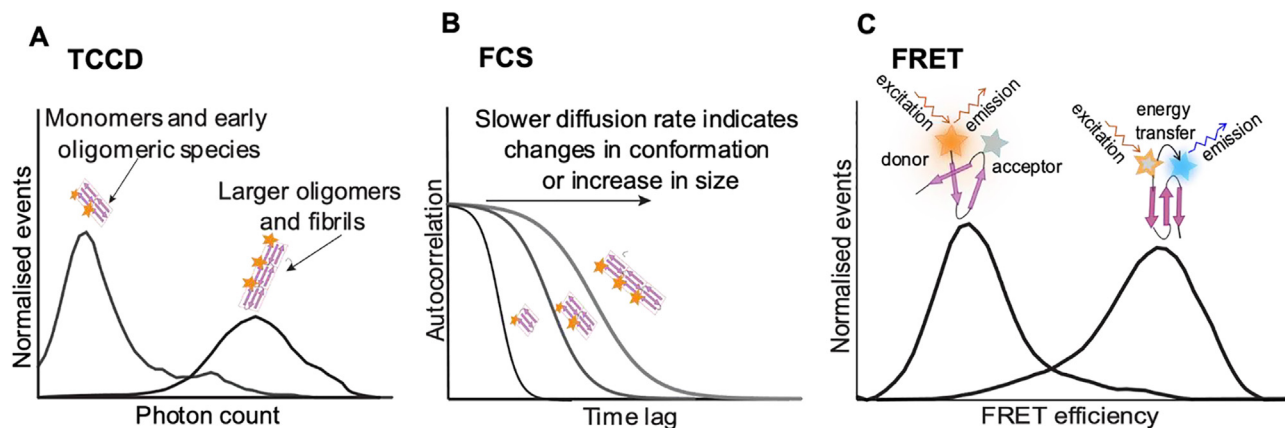
Fig. 4. The single-molecule methods of two-colour coincidence detection (TCCD), fluorescence correlation spectroscopy (FCS) and Förster resonance energy transfer (FRET). Proteins that are conjugated to a fluorophore emit fluorescence at the emission wavelength specific to the fluorophore label. (A) TCCD: Molecules diffusing through the confocal volume that change in size over time (*e.g.* during amyloid fibril formation or disaggregation) result in fluorescence burst intensities proportional to their size, and a change in the diffusion rate. These are analysed and plotted as frequency distributions for each population present. (B) FCS: The fluctuations in fluorescence observed over time can be analysed using statistical correlation functions to precisely determine changes in size of a molecule over time. (C) FRET: Proteins labelled with two FRET competent fluorophores may change in conformation, bringing the fluorophores closer together which facilitates a donor fluorophore (orange) transferring energy to an acceptor fluorophore (blue), resulting in detectable emission from the acceptor and thus an increase in FRET efficiency. In this way, the FRET efficiency can report on conformational changes in the protein. These FRET signals can be observed whilst the protein is immobilised on the surface of a coverslip for TIRF microscopy or diffusing through a confocal volume for confocal microscopy.

observations and measurements. However, by exploiting photobleaching it is possible to quantitatively characterise stoichiometries and subunit copy numbers. This is achieved by counting photobleaching steps in the signal arising from a multi-protein complex as labelled proteins bleach one by one [139]. To do so, there are several experimental requirements: proteins of interest must be labelled at a high efficiency and known labelling ratio to reduce the possibility of unlabelled protein subunits being incorporated into complexes. In addition, proteins must be immobilised at low spatial density to allow for the separate monitoring of individual proteins without signal from neighbouring complexes impacting the recorded fluorescence [140]. In order to satisfy these conditions, TIRF microscopy is the most commonly used platform for photobleaching experiments [140].

Single-molecule photobleaching has been exploited to characterise heterogeneous populations of Aβ (1-40) oligomers [141]. Gel-filtration chromatographic analysis of this population did not allow for the conclusive assignment of the size of oligomers in solution [141]. By using a single-molecule photobleaching approach, the range of oligomers in solution could be characterised, including the identification of hexameric oligomers that were not detected using gel filtration [141]. Additionally, photobleaching has been used to demonstrate that Aβ(1-40) oligomers in a heterogeneous range from monomers to hexamers are able to bind to neuroblastoma cells, with the most abundantly bound oligomeric species being dimer/tetramer complexes [142], supporting the theory that smaller oligomeric species are more cytotoxic and capable of binding cells.

Whilst single-molecule photobleaching is clearly a valuable tool for characterising protein complexes, there are some aspects that require consideration, in particular in relation to protein aggregates. For example, analysis of the time-*versus*-intensity trajectories generated during photobleaching experiments often requires selection of trajectories that have 'defined' photobleaching steps, a process that can be highly subjective [143]. Improvements to analyses of this kind are being introduced with the use of deep-learning analysis pipelines to remove the subjectivity of selecting trajectories [143]. Additionally, labelled proteins are prone to 'pre-bleaching' wherein a proportion of fluorophores bleach prior to measurements being made. This phenomenon has been corrected for previously by creating a bleaching standard using

covalently-linked fluorescently-labelled multimers [144]. The authors applied this correction to the photobleaching analysis of diabetes-associated human islet amyloid polypeptide (IAPP) in order to determine that the membrane binding affinity of amyloid peptides is in the order of trimer > dimer > tetramer ≫ monomer, in line with previous results obtained via FCS [144,145]. A similar approach could be employed to correct for the issue of fluorophore quenching, a phenomenon wherein the close proximity and altered dipole of fluorophores in large amyloid aggregates can result in the dimming of fluorescence and thus potentially resulting in an inaccurate determination of subunit counts and stoichiometries [141].

3.3.2. TCCD

Two-colour-coincidence detection (TCCD) is a fluorescence-based single-molecule method that allows quantification of the number of freely diffusing molecules in solution, and the association (including stoichiometries) between molecules [146]. These two-colour measurements rely on each biomolecule being labelled with its own distinct fluorophore, such that each fluorophore can be excited by spatially overlapped diffraction-limited, confocal laser foci [101,146] (Fig. 4A). The solution is imaged at pico-molar concentrations of fluorescent species and the signal at multiple emission wavelengths is used to detect the presence of coincident fluorescent bursts within the confocal volume; the respective fluorescent intensities can be used to determine the number of biomolecules present in a complex [77,101,119]. Dilution of samples down to the pico-molar range is required for TCCD as this decreases the likelihood of fluorescent species that are not part of a complex simultaneously traveling through the small probe volume [101,147]. The requirement of very low concentrations of the fluorescent species in TCCD is an important consideration when studying transient/weak protein–protein interactions: chemical cross-linkers may be required to capture interactions for TCCD.

The disaggregation of Aβ fibrils has been tracked using TCCD, wherein the release of fluorescently labelled oligomers and monomers of Aβ(1-40) from mature amyloid fibrils was tracked over time [148]. The observed disaggregation rates from these single-molecule experiments were in accord with estimations determined previously based on hydrogen deuterium mass spectrometry data [149]. Moreover, using this single-molecule approach it has been

demonstrated that both oligomers and monomers are released as Aβ fibrils disaggregate, as had been previously proposed, but had not been shown experimentally [150]. A TCCD approach was also used to determine the apparent size of α-syn oligomers and to observe the interconversion between toxic and non-toxic oligomeric forms of α-syn [146]. It was concluded that the median size of the most cytotoxic α-syn oligomeric form is 38 ± 10 molecules [146]. Cremades et al. (2012) [77] combined TCCD experiments with cell-based experiments in order to correlate the size of the oligomers with their cytotoxicity. However, it remains challenging to accurately determine fibril lengths using TCCD; this is partly due to the requirement of careful thresholding of the signal in order to define true events as opposed to background noise [101]. If this threshold is set too low, the fluctuations in noise from the instrument itself can result in false event detection [101]. Thus, the possibility arises that TCCD may not be capable of accurately determining the size of the smallest species formed early during the aggregation process [146]. In contrast, the length of smaller oligomeric species can be readily obtained via a TIRF microscopy approach, using labelled protein monomers (with one fluorophore per monomer) (as depicted in Fig. 3A). This measurement gives an absolute value of units of length within smaller oligomeric species by dividing the total fluorescence intensity by the intensity of one fluorophore, or the intensity of a photobleaching step [151]. A combination of both methods of measurement may be required to fully characterise the heterogeneous species present in solution. These quantitative measurements have been used for an analysis of the effect of oligomer size on the generation of reactive oxygen species and membrane permeability upon binding to neuronal cells [119,123].

3.3.3. FCS

Fluorescence correlation spectroscopy (FCS) is a statistical technique commonly coupled to confocal microscopy which facilitates in-depth analysis of particles diffusing through the confocal volume [102,152–154] (Fig. 4B). To perform FCS, a solution of fluorescently-labelled molecules are imaged at a concentration that corresponds to a small number [155] of molecules (~1) being present in the detection volume simultaneously: data on the transient, statistical fluctuations in the fluorescence are collected and compared to rapid changes in the fluorescence attributable to 'noise' in the signal [153,156]. The fluctuations in fluorescence intensity can be analysed and assigned to a specific feature of the molecule using mathematical auto- or cross- correlation models [157]. This analysis uses the 'diffusion time' of a molecule to extract the size, conformation, concentration and chemical kinetic rate constants of the molecules and processes in question [157]. The hydrodynamic radius, a geometric parameter of a polymer in solution, can be used in this context as an indicator of the amount of movement of the detected proteins. An important consideration when utilising FCS is that proteins in a more spherical conformation will have a smaller hydrodynamic radii as opposed to those with a non-spherical structure [158]; whilst the hydrodynamic radius is a useful parameter for examining conformational changes, it can be difficult to ascertain whether a change in diffusion is due to a change in the molecular mass or the shape of the diffusing molecule. The complexity of the types of FCS experiments that can be performed has increased over the years, such that now proteins can be labelled with different coloured fluorescent probes in order to detect protein–protein interactions (indicative of complex or aggregate formation). Multi-colour cross-correlation analysis of bimolecular associations (referred to as FCCS, fluorescence cross-correlation spectroscopy) is useful for studying multi-component protein complexes.

Recently, Li et al. (2019) employed both FCS and FCCS to detect small differences in the size of α-syn oligomers and highlight the potential role of oligomers in the early aggregation process. Engineered tandem α-syn oligomers of specific sizes (monomers, dimers, tetramers, and octamers) were labelled in equimolar amounts with two different fluorophores, and then aggregated. At time points during the early aggregation process, FCCS was performed to determine which associations were most likely to occur [160]. It was found that early-stage oligomeric α-syn forms fibrils by self-associating with other oligomers at a faster rate and to a greater extent than with free monomers, suggesting that the well-established impact of oligomers on the rate and extent of mature fibril formation may be due to them requiring less conformational rearrangement to add to the growing fibrils compared to monomers [161–164]. This result highlights the capacity of techniques with the sensitivity of FCCS to uncover mechanistic details of heterogeneous systems such as those formed during the early stages of amyloid fibril formation.

Protein aggregation can be followed by FCS by comparing diffusion rates and thus the hydrodynamic radii of species as the aggregates grow in size or change in conformation [165–169]. By using FCS to detect the changes in the size and conformation of early-stage Aβ(1-42) aggregates over a range of concentrations it was determined that a critical oligomerisation concentration of 90 nM exists for this peptide [170]. Oligomers with an average size of ~ 50 monomeric units and an elongated conformation, consistent with a protofibril, were observed at this critical concentration point [170]. Identifying conformational states and the concentrations at which cytotoxic oligomers form is an essential step towards developing novel therapeutics and early detection methods for diseases associated with amyloid fibril formation.

FCCS can be combined with advanced excitation regimes for improved accuracy in detecting multiple fluorescent wavelengths in the same sample. Alternating laser excitation (ALEX)-FCCS involves alternating the laser excitation wavelength on a microsecond timescale and facilitates detection of multiple fluorescent species without spectral crosstalk interfering with the accuracy of the measurements, without the need for multiple detection channels [171,172]. This concept has been advanced by pulsed interleaved excitation (PIE) wherein the laser excitation is alternated on the nanosecond timescale, enabling multiple fluorophores to be excited within the time it takes for molecules to diffuse through the confocal volume [173,174]. Thus, when coupled with FCCS, PIE facilitates the detection of multiple fluorophores in a single-detection channel, and removes spectral crosstalk in a multi-channel detection system which improves the accuracy of cross-correlation functions [174]. The technical details surrounding ALEX/PIE are described in depth elsewhere [172,174]. There have been several studies that have exploited these experimental approaches to investigate amyloid fibrils. For example, early oligomerisation kinetics and size distributions of a model amyloid forming protein α-spectrin SH3 have been characterised using PIE-FCS [175]. By co-aggregating differentially labelled α-spectrin SH3 and using PIE-FCS to observe and autocorrelate coincident events, the oligomeric distribution could be determined at each time point. This experiment was able to show the gradual appearance of a heterogeneous population of early-stage soluble oligomers, leading to the suggestion that some amyloid oligomers are unable to increase in size over time [175]. ALEX/PIE extend the capability of FCS and FCCS to probe the interaction between amyloid fibrils and the proteins they interact with, as well as the complex early stages of oligomerisation that have proven otherwise difficult to accurately characterise.

3.3.4. FRET

Fluorescence resonance energy transfer (FRET) is a photophysical phenomenon wherein energy is transferred from an excited-state donor fluorophore to an acceptor fluorophore by non-

radiative dipole–dipole coupling (Fig. 4C), an effect that is inversely proportional to the distance between the donor and the acceptor (~10–100 Å, depending on the FRET pair used, referred to as the Förster distance) [176]. A large number of fluorophore pairs that exhibit FRET have been characterised, and suitable pairs can be selected to label proteins of interest depending on the type of information to be gathered (Fig. 4C) [177]. For example, FRET pairs can be used to label a single protein in two locations, such that when the protein is correctly folded, the FRET efficiency is high due to the fluorophores being in close proximity: when the protein is unfolded the FRET efficiency is lower due to the fluorophores being further apart [178]. Alternatively, to investigate protein–protein interactions, two separate proteins of interest can be labelled, each with one member of a FRET pair. High FRET efficiency would be expected if the proteins interact (and hence the FRET pair are in close proximity), and changes in FRET can be used to follow the dynamics of binding and dissociation [178].

FRET is a widely used approach for studying single molecules as it can be observed using both TIRF and confocal microscopy approaches [179,180]. TIRF microscopy allows FRET from a single molecule to be measured through time, and thus kinetic information pertaining to molecular associations (including on and off rates) or changes in protein conformation can be elucidated [181,182]. Alternatively, when used in conjunction with a confocal approach, FRET can report on molecular diffusion in tandem with protein-interactions. Such an approach avoids problems with steric hindrance that can occur as a result of the surface immobilisation required for TIRF microscopy [183,184].

In recent years, several studies have utilised FRET as a technique to characterise oligomeric α-syn [76–78]. Well-characterised FRET pairs (such as AlexaFluor488 and AlexaFluor555 fluorophores) can be conjugated in equimolar amounts to monomeric α-syn, and the FRET efficiency measured in order to deduce precisely how monomers interact with one another during the early stages of the aggregation process. In these cases, a higher FRET efficiency is indicative of a closer proximity between molecules, or an altered dipole orientation of the fluorophore indicating larger or more compact oligomers [46]. Using a confocal single-molecule FRET approach, two structurally distinct oligomeric species of α-syn have been detected (named Type A and Type B) one of which is more compact and cytotoxic (Type B) [78]. The interconversion between these two species has been kinetically defined by measuring the transitions between FRET states, and this transition is the rate-limiting step in the formation of mature fibrils. The formation of mature fibrils following the transition to Type B is rapid, whilst the transition from Type A to Type B is slow [78]. This transition process may be a cyto-protective mechanism: it results in the burial of the exposed hydrophobic (and thus damaging) residues present in Type B oligomers. The proportion of each morphologically distinct oligomeric species was determined for a Parkinson's disease-associated mutant form of α-syn [78]. The class of oligomer rapidly formed by A53T α-syn was the Type B oligomer, consistent with previous studies utilising ensemble-based approaches that have shown more rapid oligomerisation for this mutant [43]. In contrast, Type A oligomers predominated during the early stages of the aggregation of A30P mutant of α-syn, consistent with the finding that fibril formation is slower for the A30P mutant of α-syn [43,185]. Thus, by using a confocal microscopy single-molecule FRET based approach, Tosatto et al. (2015) rationalised the kinetics of α-syn oligomerisation and provided unprecedented insight into the molecular mechanism that drives this disease-related process [78].

The functional yeast prion protein Ure2 also readily forms amyloid fibrils [186], and both oligomerisation and disaggregation of this protein have been investigated using combined TIRF and confocal single-molecule FRET approaches [46]. Conjugating donor and acceptor fluorophores in site-specific locations on the protein (chosen based on their expected Förster distance and dipole orientation upon β-sheet formation) showed that a conversion between oligomeric species is the rate-limiting step in the progression from soluble oligomers to amyloid fibrils. In particular, increasing FRET values over time suggested a more compact oligomer is present immediately prior to fibril elongation. This transition to a more compact state is invisible in ensemble biochemistry techniques as it occurs within the 'lag' phase (prior to ThT increasing in fluorescence during the exponential growth phase). The disaggregation of Ure2 [46] and α-syn [77] has also been examined using a single-molecule FRET approach. Oligomeric species released from mature fibrils of both proteins have FRET values that mirror those of species detected immediately prior to amyloid fibril elongation, suggesting that disaggregation results in on-pathway species that could propagate further fibril formation.

4. Studying the interaction of aggregates with other proteins using fluorescence-based single-molecule techniques

Single-molecule fluorescence methods can be used to detect protein–protein interactions involved in some of the most complex molecular processes that underpin life and disease states. This includes membrane-protein interactions involved in cell-signalling processes [187,188], and DNA-replication machinery [189]. A key example of a cellular process that uniquely benefits from such approaches is the interplay between protein aggregates and molecular chaperones.

In order to avoid the formation of toxic protein aggregates, cells employ a number of protein quality control mechanisms, including molecular chaperones, which engage with destabilised proteins in order to prevent them from aggregating (for more detailed reviews on the mechanism of action of molecular chaperones, see [190,191]). Moreover, molecular chaperones have been found to co-localise with amyloid fibrils within the proteinaceous inclusions in the neurons of patients with neurodegenerative diseases [192–196]. However, the interaction between molecular chaperones and amyloid fibril forming proteins can be difficult to characterise using bulk biochemical techniques owing to the highly heterogeneous and dynamic nature of both systems [190]. As a consequence, single-molecule fluorescence approaches have been invaluable in elucidating the interactions between molecular chaperones and amyloid fibril forming proteins.

The aggregation of the protein tau is associated with a number of neurodegenerative diseases, most notably Alzheimer's disease. By conjugating a donor fluorophore (AlexaFluor488) to tau, and an acceptor (AlexaFluor647) to the ATP-dependent chaperone Hsp70, interactions between these two species could be detected by FRET [197]. This approach enabled the size of both Hsp70 and the tau aggregates in samples to be determined and the dissociation rate of Hsp70 from different tau species to be determined. In doing so, this study established that Hsp70 binds to and then rapidly dissociates from tau monomers, yet forms increasingly stable binding interactions with oligomers and fibrils of tau (as a function of aggregate size).

A study by Cox et al. (2018) examined the binding of small heat shock proteins (sHsp) to α-syn fibrils by using the widely available AIE dyes ThT and Nile red, as well as AlexaFluor647 conjugated to the ATP-independent sHsp Hsp27 [112]. Using TIRF microscopy with dual excitation, individual α-syn fibrils were visualised by the emission of the ThT dye (at 480 nm) and the localisation of Hsp27 on the fibrils established by the emission at 670 nm. This work demonstrated that Hsp27 forms stable complexes with α-syn fibrils. Moreover, by using Nile Red in place of ThT for the imaging of the fibrils, it was demonstrated that the fibrils bound

by Hsp27 had reduced surface hydrophobicity and this correlated with reduced cytotoxicity of the Hsp27-coated fibrils [112]. Whilst single-molecule fluorescence microscopy has enhanced the ability to observe stable interactions between sHsps and amyloid fibrils, there is still very little known about the specific mechanisms responsible for sHsp chaperone function. Moreover, there has been wide speculation on the precise role of the various oligomeric forms of sHsps when it comes to interacting with fibrils [198–200]. Recently, this type of mechanistic detail has been investigated using single-molecule photobleaching in the context of a protein that forms amorphous aggregates [201]; a similar experimental approach could be employed to study the interaction of sHsps with amyloid fibrils.

The extracellular chaperone clusterin can bind to and reduce the toxicity of oligomeric forms of α-syn [202]. By labelling α-syn and clusterin with AlexaFluor488 and AlexaFluor647 (respectively), Whiten et al. (2018) followed the interaction of these two proteins by TCCD under conditions that promote α-syn aggregation. Supported by ensemble-based enzyme-linked immunosorbent assays, this single-molecule work determined the apparent stoichiometry of clusterin bound to α-syn over time by comparing the relative fluorescence of coincident bursts within the confocal volume. During the aggregation of α-syn, the amount of clusterin that was bound to α-syn reduced as the size of the α-syn oligomers increased. From this it was concluded that clusterin binds to hydrophobic regions on the surface of α-syn fibrils: as the aggregation of α-syn proceeds the surface hydrophobicity of fibrils decreases and this leads to a decrease in the amount of bound clusterin.

Apolipoprotein E (ApoE) has been found within Aβ plaques in the brains of patients with AD [203,204], and mutations in the gene encoding ApoE (the polymorphic ε2, ε3, and ε4 *APOE* alleles) increase the severity and likelihood of both early and late onset forms of AD (in particular the ε4 allele (ApoE4), which is the strongest risk factor for AD) [205] (reviewed in depth elsewhere, see [159]). Both ALEX-FCCS and FCS have been used to detect complexes formed between Aβ(1-40), ApoE3 and ApoE4 [206]. By labelling the ApoE mutants and Aβ(1-40) with AlexaFluor488 and AlexaFluor647 respectively, and analysing their diffusion on a confocal microscope using alternating laser excitation to reduce fluorophore cross-talk [174], fluorescence fluctuations were cross-correlated and analysed for the presence of complexes. An association between the two proteins was established using this method, suggesting that there is an interaction between Aβ(1-40) and ApoE [206]. Furthermore, the auto-correlation of Aβ during amyloid formation showed the species formed had a smaller hydrodynamic radius in the presence of both ApoE mutants compared to when ApoE was not present. This suggests that by forming complexes with Aβ, ApoE reduces the size of the Aβ aggregates. Interestingly, this effect on the size of the Aβ aggregates was reduced in the presence of ApoE4 compared to ApoE3, suggesting that the increased risk of disease associated with this mutation is due to a decrease in the capacity of ApoE to bind Aβ(1-40) and inhibit amyloid fibril formation. This result provides compelling evidence as to how mutations in ApoE may increase the risk and severity of AD. Moreover, the use of ALEX-FCCS and FCS in this work highlights how single-molecule fluorescence techniques can be used to uncover molecular mechanisms that relate to the onset and progression of diseases associated with amyloid fibril formation. Elucidating the details of these dynamic biomolecular associations is not possible using post-mortem tissues from patients [207,208].

The disaggregation of tau [69] and α-syn [209,210] fibrils by the Hsp70 system has been previously documented *in vitro*; however, a detailed mechanistic model for this process remained to be established. Recently, the disaggregation of α-syn by the Hsp70 disaggregase system has been studied using ensemble-averaged FRET, fluorescence anisotropy, and kinetic monte-carlo simulations [68].

This work proposed a model in which the Hsp40 co-chaperone selectively binds oligomeric forms of α-syn in order to sequester Hsp70 onto amyloid structures, in turn facilitating entropic pulling via molecular crowding of the chaperones [68]. This mechanism was established by labelling equimolar amounts of Hsp70 molecules with a FRET pair such that, if crowding of Hsps70 molecules on the α-syn fibril occurred, the FRET efficiency would be high. In contrast, if the Hsp70 molecules were spread out along the fibril, the FRET efficiency would be low. Furthermore, a more dramatic increase in FRET efficiency in the presence of the NEF Hsp110 demonstrated that Hsp110 acts to increase the propensity for molecular crowding of Hsp70, enhancing entropic pulling. This mechanistic model provides evidence for a previously proposed theory that entropic pulling is responsible for the depolymerisation or fragmentation of amyloid fibrils [211,212]. Conclusive evidence for this mechanistic model could be provided by using TIRF-based experiments, including fluorophore photobleaching to directly observe and quantify molecular crowding, the position on the fibril at which this occurs, and the binding and dissociation rates of Hsp70/40 and NEF Hsp110. Moreover, the discovery of new AIE dyes with large Stokes shifts, such as ASCP [88,108] provide the possibility to visualise fibrils and proteins that interact with them using only one excitation source [108]. More complex three-colour fluorescence experiments would enable more components to be observed simultaneously [213,214] and thus be invaluable for the study of how chaperone machines, such as how the Hsp70/Hsp40/Hsp110 disaggregase system [66,75], interact with amyloid fibrils.

5. Summary and outlook

This review has focussed on the use of single-molecule fluorescence-based approaches for the study of the molecular details underpinning amyloid fibril formation and their interaction with other proteins, in particular molecular chaperones. Understanding mechanistic details of the oligomerisation process, as well as the protein–protein interactions that interfere with it, is an important step towards the development of novel drugs to treat or even prevent diseases such as Alzheimer's and Parkinson's disease. As a result of being highly heterogeneous, some of the mechanistic details of amyloid fibril formation are difficult to ascertain using ensemble-based techniques. Single-molecule fluorescence methods, such as TCCD, FCS and FRET, have already provided insight into these dynamic and heterogeneous processes. Recent work on the mechanism by which molecular chaperones bind to fibrils [112,119,197,206], and the species released during the disaggregation of fibrils [74,149] are excellent examples of this. However, there is still considerable scope to apply and extend these single-molecule methods for the study of fibrils and the manner in which they interact with other proteins.

Finally, it is important to recognise that these single-molecule fluorescence-based methods are most powerful when used in combination with other complimentary approaches. For example, techniques such as solid-state or hydrogen–deuterium exchange NMR or electron microscopy, can provide information about the structural polymorphisms of amyloid fibrils, and the impact of fluorescent tagging on these structures. It will be through the use of highly integrated approaches such as these that we will gain further fundamental knowledge that is critical to our understanding of how neurodegenerative diseases arise, and how we may interfere with this process in order to treat or prevent them.

CRediT authorship contribution statement

Lauren J. Rice: Conceptualization, Investigation, Writing – original draft, Visualization, Writing - review & editing. **Heath Ecroyd:**

Conceptualization, Project administration, Writing - review & editing. **Antoine M. van Oijen:** Conceptualization, Project administration, Writing - review & editing.

Declaration of Competing Interest

The authors declare that they have no known competing financial interests or personal relationships that could have appeared to influence the work reported in this paper.

References

[1] Wang W, Nema S, Teagarden D. Protein aggregation-pathways and influencing factors. Int J Pharmaceut 2010;390:89–99.

[2] Anfinsen CB. Principles that govern the folding of protein chains. Science 1973;181(4096):223–30.

[3] Fink AL. Protein aggregation: folding aggregates, inclusion bodies and amyloid. Fold Design 1998;3(1):R9–R23.

[4] Jahn TR, Radford SE. Folding versus aggregation: polypeptide conformations on competing pathways. Arch Biochem Biophys 2008;469(1):100–17.

[5] Hendrick JP, Hartl FU. Molecular chaperone functions of heat-shock proteins. Annu Rev Biochem 1993;62:349–84.

[6] Hendrick JP, Hartl FU. The role of molecular chaperones in protein folding. FASEB J 1995;9(15):1559–69. https://doi.org/10.1096/fasebj.9.15.8529835.

[7] Terry RD, Gonatas NK, Weiss M. Ultrastructural studies in Alzheimer's presenile dementia. Am J Pathol 1964;44(2):269–97.

[8] Serpell LC. Alzheimer's amyloid fibrils: structure and assembly. Biochim Biophys Acta (BBA) – Mol Basis Dis 2000;1502(1):16–30.

[9] Polymeropoulos MH et al. Mutation in the alpha-synuclein gene identified in families with Parkinson's disease. Science 1997;276(5321):2045–7.

[10] Chiti F, Dobson CM. Protein misfolding, amyloid formation, and human disease: a summary of progress over the last decade. Annu Rev Biochem 2017;86:27–68.

[11] Chiti F, Dobson CM. Protein misfolding, functional amyloid, and human disease. Annu Rev Biochem 2006;75(1):333–66.

[12] Elsasser WM. Outline of a theory of cellular heterogeneity. Proc Natl Acad Sci USA 1984;81(16):5126–9.

[13] Bacic L, Sabantsev A, Deindl S. Recent advances in single-molecule fluorescence microscopy render structural biology dynamic. Curr Opin Struct Biol 2020;65:61–8.

[14] Young G et al. Quantitative mass imaging of single biological macromolecules. Science 2018;360(6387):423.

[15] Shashkova S, Leake MC. Single-molecule fluorescence microscopy review: shedding new light on old problems. Biosci Rep 2017;37(4). https://doi.org/10.1042/BSR20170031.

[16] Giese A et al. Single particle detection and characterization of synuclein co-aggregation. Biochem Biophys Res Commun 2005;333(4):1202–10.

[17] van Oijen AM. Single-molecule approaches to characterizing kinetics of biomolecular interactions. Curr Opin Biotechnol 2011;22(1):75–80.

[18] Monachino E, Spenkelink LM, van Oijen AM. Watching cellular machinery in action, one molecule at a time. J Cell Biol 2016;216(1):41–51.

[19] Dovidchenko NV, Leonova EI, Galzitskaya OV. Mechanisms of amyloid fibril formation. Biochemistry Biokhimiia 2014;79(13):1515–27.

[20] Nelson R et al. Structure of the cross-β spine of amyloid-like fibrils. Nature 2005;435(7043):773–8.

[21] Gallardo R, Ranson NA, Radford SE. Amyloid structures: much more than just a cross-β fold. Curr Opin Struct Biol 2020;60:7–16.

[22] Falcon B et al. Novel tau filament fold in chronic traumatic encephalopathy encloses hydrophobic molecules. Nature 2019;568(7752):420–3.

[23] Sawaya MR et al. Atomic structures of amyloid cross-β spines reveal varied steric zippers. Nature 2007;447(7143):453–7.

[24] Naiki H, Higuchi K, Hosokawa M, Takeda T. Fluorometric determination of amyloid fibrils in vitro using the fluorescent dye, thioflavine T. Anal Biochem 1989;177(2):244–9.

[25] Amdursky N, Erez Y, Huppert D. Molecular Rotors: what lies behind the high sensitivity of the Thioflavin-T fluorescent marker. Acc Chem Res 2012;45(9):1548–57.

[26] Nielsen L et al. Effect of environmental factors on the kinetics of insulin fibril formation: elucidation of the molecular mechanism. Biochemistry 2001;40(20):6036–46.

[27] Wood SJ, Wypych J, Steavenson S, Louis JC, Citron M, Biere AL. alpha-synuclein fibrillogenesis is nucleation-dependent. Implications for the pathogenesis of Parkinson's disease. J Biol Chem 1999;274(28):19509–12.

[28] Narkiewicz J, Giachin G, Legname G. In vitro aggregation assays for the characterization of α-synuclein prion-like properties. Prion 2014;8(1):19–32.

[29] Yu CYY, Zhang W, Kwok RTK, Leung CWT, Lam JWY, Tang BZ. A photostable AIEgen for nucleolus and mitochondria imaging with organelle-specific emission. J MaterChem B 2016;4(15):2614–9.

[30] Buell AK et al. Solution conditions determine the relative importance of nucleation and growth processes in α-synuclein aggregation. Proc Natl Acad Sci 2014;111(21):7671–6.

[31] Jiménez JL, Nettleton EJ, Bouchard M, Robinson CV, Dobson CM, Saibil HR. The protofilament structure of insulin amyloid fibrils. Proc Natl Acad Sci USA 2002;99(14):9196–201.

[32] Meinhardt J, Sachse C, Hortschansky P, Grigorieff N, Fändrich M. Aβ(1–40) fibril polymorphism implies diverse interaction patterns in amyloid fibrils. J Mol Biol 2009;386(3):869–77.

[33] Close W et al. Physical basis of amyloid fibril polymorphism. Nat Commun 2018;9(1):699.

[34] Kreplak L, Aebi U. From the polymorphism of amyloid fibrils to their assembly mechanism and cytotoxicity. Adv Protein Chem 2006;73:217–33.

[35] Periole X et al. Energetics underlying twist polymorphisms in amyloid fibrils. J Phys Chem B 2018;122(3):1081–91.

[36] Fitzpatrick AWP, Saibil HR. Cryo-EM of amyloid fibrils and cellular aggregates. Curr Opin Struct Biol 2019;58:34–42.

[37] Gremer L et al. Fibril structure of amyloid-β(1–42) by cryo–electron microscopy. Science 2017;358(6359):116–9.

[38] Li Y-W et al. Amyloid fibril structure of α-synuclein determined by cryo-electron microscopy. Cell Res 2018;28(07/31.

[39] Zarranz JJ et al. The new mutation, E46K, of alpha-synuclein causes Parkinson and Lewy body dementia. Ann Neurol 2004;55(2):164–73.

[40] Rutherford NJ, Moore BD, Golde TE, Giasson BI. Divergent effects of the H50Q and G51D SNCA mutations on the aggregation of α-synuclein. J Neurochem 2014;131(6):859–67.

[41] Kollmer M et al. Cryo-EM structure and polymorphism of Aβ amyloid fibrils purified from Alzheimer's brain tissue. Nat Commun 2019;10(1):4760M. Kollmer et al., "Cryo-EM structure and polymorphism of Aβ amyloid fibrils purified from Alzheimer's brain tissue," Nature Communications, vol. 10, no. 1, p. 4760, 2019/10/29 2019..

[42] Winner B et al. In vivo demonstration that α-synuclein oligomers are toxic. Proc Natl Acad Sci 2011;108(10):4194–9.

[43] Conway KA, Lee SJ, Rochet JC, Ding TT, Williamson RE, Lansbury Jr PT. Acceleration of oligomerization, not fibrillization, is a shared property of both alpha-synuclein mutations linked to early-onset Parkinson's disease: implications for pathogenesis and therapy. Proc Natl AcadSci USA 2000:571–6.

[44] Dear AJ et al. Identification of on- and off-pathway oligomers in amyloid fibril formation. Chem Sci 2020;11(24):6236–47. https://doi.org/10.1039/C9SC06501F.

[45] Dear AJ et al. Kinetic diversity of amyloid oligomers. Proc Natl Acad Sci USA 2020;11722:12087–94.

[46] Yang J et al. Direct observation of oligomerization by single molecule fluorescence reveals a multistep aggregation mechanism for the yeast prion protein Ure2. J Am Chem Soc 2018;140(7):2493–503.

[47] Trovato A, Chiti F, Maritan A, Seno F. Insight into the structure of amyloid fibrils from the analysis of globular proteins. PLoS Comput Biol 2006;2(12):e170.

[48] Cohen SIA, Vendruscolo M, Dobson CM, Knowles TPJ. Nucleated polymerization with secondary pathways. II. Determination of self-consistent solutions to growth processes described by non-linear master equations. J Chem Phys 2011;135(6):065106.

[49] Cohen SIA, Linse S, Luheshi LM, Hellstrand E, White DA, Rajah L, et al. Proliferation of amyloid-β42 aggregates occurs through a secondary nucleation mechanism. Proc Natl Acad Sci USA 2013;11024:9758–63.

[50] Michaels TCT, Lazell HW, Arosio P, Knowles TPJ. Dynamics of protein aggregation and oligomer formation governed by secondary nucleation. J Chem Phys 2015;143(5):054901.

[51] Verma M, Vats A, Taneja V. Toxic species in amyloid disorders: oligomers or mature fibrils. Ann Indian Acad Neurol 2015;18(2):138–45.

[52] Linse S. Monomer-dependent secondary nucleation in amyloid formation. Biophys Rev 2017;9(4):329–38.

[53] Thacker D, Sanagavarapu K, Frohm B, Meisl G, Knowles TPJ, Linse S. The role of fibril structure and surface hydrophobicity in secondary nucleation of amyloid fibrils. Proc Natl Acad Sci USA 2020;11:25272–83.

[54] Bunce SJ, Wang Y, Stewart KL, Ashcroft AE, Radford SE, Hall CK, et al. Molecular insights into the surface-catalyzed secondary nucleation of amyloid-β40 (Aβ40) by the peptide fragment Aβ16–22. Sci Adv 2019;5(6):eeav8216.

[55] Peduzzo A, Linse S, Buell AK. The properties of α-synuclein secondary nuclei are dominated by the solution conditions rather than the seed fibril strain. ACS Chem Neurosci 2020;11(6):909–18.

[56] Aprile FA et al. Selective targeting of primary and secondary nucleation pathways in Aβ42 aggregation using a rational antibody scanning method. Sci Adv 2017;3(6):e1700488.

[57] Knowles TPJ, Vendruscolo M, Dobson CM. The amyloid state and its association with protein misfolding diseases. Nat Rev Mol Cell Biol 2014;15(6):384–96.

[58] Xue WF, Hellewell AL, Hewitt EW, Radford SE. Fibril fragmentation in amyloid assembly and cytotoxicity: when size matters. Prion 2010;4(1):20–5.

[59] Knowles TPJ et al. An analytical solution to the kinetics of breakable filament assembly. Science 2009;326(5959):1533–7.

[60] Kundel F et al. Measurement of Tau filament fragmentation provides insights into prion-like spreading. ACS Chem Neurosci 2018;9(6):1276–82.

[61] Beal DM, Tournus M, Marchante R, Purton TJ, Smith DP, Tuite MF. The division of amyloid fibrils: systematic comparison of fibril fragmentation stability by linking theory with experiments. iScience 2020;23(9):101512.

[62] Hill TL. Length dependence of rate constants for end-to-end association and dissociation of equilibrium linear aggregates. Biophys J 1983;44(2):285–8.

[63] Tarutani A et al. The effect of fragmented pathogenic α-synuclein seeds on prion-like propagation. J Biol Chem 2016;291(36):18675–88.

[64] Sternke-Hoffmann R, Peduzzo A, Bolakhrif N, Haas R, Buell AK. The aggregation conditions define whether EGCG is an inhibitor or enhancer of α-synuclein amyloid fibril formation. Int. J. Mol. Sci. 2020;21(6).

[65] Linse S. Mechanism of amyloid protein aggregation and the role of inhibitors. Pure Appl Chem 2019;91(2):211–29.

[66] Shorter J. Hsp104: A weapon to combat diverse neurodegenerative disorders. Neurosignals 2008;16(1):63–74.

[67] Glover JR, Lindquist S. Hsp104, Hsp70, and Hsp40: A novel chaperone system that rescues previously aggregated proteins. Cell 1998;94(1):73–82.

[68] Wentink AS et al. Molecular dissection of amyloid disaggregation by human HSP70. Nature 2020;587(7834):483–8.

[69] Nachman E et al. Disassembly of Tau fibrils by the human Hsp70 disaggregation machinery generates small seeding-competent species. J Biol Chem 2020;295(28):9676–90.

[70] Gao X et al. Human Hsp70 disaggregase reverses parkinson's-linked α-synuclein amyloid fibrils. Mol Cell 2015;59(5):781–93.

[71] Shorter J. Engineering therapeutic protein disaggregases. Mol Biol Cell 2016;27(10):1556–60.

[72] Taguchi YV et al. Hsp110 mitigates α-synuclein pathology in vivo. Proc Natl Acad Sci 2019;116(48):24310.

[73] Jackrel ME, Shorter J. Protein-remodeling factors as potential therapeutics for neurodegenerative disease. Front Neurosci. Rev. 2017;11(99).

[74] Tittelmeier J et al. The HSP110/HSP70 disaggregation system generates spreading-competent toxic α-synuclein species. EMBO J 2020;39(13): e103954.

[75] Shorter J. The mammalian disaggregase machinery: Hsp110 synergizes with Hsp70 and Hsp40 to catalyze protein disaggregation and reactivation in a cell-free system. PLoS ONE 2011;6(10):e26319.

[76] Horrocks MH et al. Fast flow microfluidics and single-molecule fluorescence for the rapid characterization of α-synuclein oligomers. Anal Chem 2015;87 (17):8818–26.

[77] Cremades N et al. Direct observation of the interconversion of normal and toxic forms of α-synuclein. Cell 2012;149(5):1048–59.

[78] Tosatto L et al. Single-molecule FRET studies on alpha-synuclein oligomerization of Parkinson's disease genetically related mutants. Sci Rep 2015;5(1):16696.

[79] Narayan P, Meehan S, Carver JA, Wilson MR, Dobson CM, Klenerman D. Amyloid-β oligomers are sequestered by both intracellular and extracellular chaperones. Biochemistry 2012;51(46):9270–6.

[80] Sunde M, Blake C. The structure of amyloid fibrils by electron microscopy and X-ray diffraction. Adv Protein Chem 1997;50:123–59.

[81] Stefani M. Structural polymorphism of amyloid oligomers and fibrils underlies different fibrillization pathways: immunogenicity and cytotoxicity. Curr Protein Peptide Sci 2010;11:343–54.

[82] Meade RM, Fairlie DP, Mason JM. Alpha-synuclein structure and Parkinson's disease – lessons and emerging principles. Mol Neurodegener 2019;14(1):29.

[83] Strohäker T et al. Structural heterogeneity of α-synuclein fibrils amplified from patient brain extracts. Nat Commun 2019;10(1):5535.

[84] Cecconi C, Shank EA, Bustamante C, Marqusee S. Direct observation of the three-state folding of a single protein molecule. Science 2005;309 (5743):2057.

[85] Lu HP, Xun L, Xie XS. Single-molecule enzymatic dynamics. Science 1998;282 (5395):1877.

[86] Castello F et al. Two-step amyloid aggregation: sequential lag phase intermediates. Sci Rep 2017;7(1):40065.

[87] Yokota H. Fluorescence microscopy for visualizing single-molecule protein dynamics. Biochim Biophys Acta, Gen Subj 2020;1864(2):129362.

[88] Hong Y, Lam J, Tang B. Aggregation-induced emission. Chem Soc Rev 2011;40 (11):5361–88.

[89] Luo J et al. Aggregation-induced emission of 1-methyl-1,2,3,4,5-pentaphenylsilole. Chem Commun 2001;18:1740–1.

[90] Conway KA, Harper JD, Lansbury PT. Accelerated in vitro fibril formation by a mutant α-synuclein linked to early-onset Parkinson disease. Nat Med 1998;4 (11):1318–20.

[91] Hijaz BA, Volpicelli-Daley LA. Initiation and propagation of α-synuclein aggregation in the nervous system. Mol Neurodegener 2020;15(1):19.

[92] Smith CL. Basic confocal microscopy. Curr Protoc Mol Biol 2008;81 (1):14.11.1–14.11.18.

[93] Datta R, Heaster TM, Sharick JT, Gillette AA, Skala MC. Fluorescence lifetime imaging microscopy: fundamentals and advances in instrumentation, analysis, and applications. J Biomed Opt 2020;25(7):1–43.

[94] Wilson T. Confocal Microscopy. In: Guenther BD, Steel DG, editors. Encyclopedia of Modern Optics (Second Edition). Oxford: Elsevier; 2005. p. 194–202.

[95] Neil MAA, Juškaitis R, Wilson T. Method of obtaining optical sectioning by using structured light in a conventional microscope. Opt Lett 1997;22 (24):1905–7.

[96] Thiele JC et al. Confocal fluorescence-lifetime single-molecule localization microscopy. ACS Nano 2020;14(10):14190–200.

[97] Nie S, Chiu DT, Zare RN. Real-time detection of single molecules in solution by confocal fluorescence microscopy. Anal Chem 1995;67(17):2849–57.

[98] Castello M, Tortarolo G, Buttafava M, et al. A robust and versatile platform for image scanning microscopy enabling super-resolution FLIM. Nat Methods 2019;16:175–8. https://doi.org/10.1038/s41592-018-0291-9.

[99] Fish KN. Total Internal Reflection Fluorescence (TIRF) Microscopy. Current Protocols in Cytometry 2009;50:12.18.1–12.18.13.

[100] Llères D, Bailly AP, Perrin A, Norman DG, Xirodimas DP, Feil R. Quantitative FLIM-FRET microscopy to monitor nanoscale chromatin compaction in vivo reveals structural roles of condensin complexes. Cell Rep 2017;18 (7):1791–803.

[101] Orte A, Clarke R, Klenerman D. Single-molecule two-colour coincidence detection to probe biomolecular associations. Biochem Soc Trans 2010;38 (4):914–8.

[102] Jazani S, Sgouralis I, Shafraz OM, Levitus M, Sivasankar S, Pressé S. An alternative framework for fluorescence correlation spectroscopy. Nat Commun 2019;10(1):3662.

[103] Axelrod D, Thompson NL, Burghardt TP. Total internal inflection fluorescent microscopy. J Microsc 1983;129(1):19–28.

[104] Sako Y, Uyemura T. Total internal reflection fluorescence microscopy for single-molecule imaging in living cells. Cell Struct Funct 2002;27(5):357–65.

[105] Crites T.J., Chen L., Varma R., A TIRF microscopy technique for real-time, simultaneous imaging of the TCR and its associated signaling proteins; J Vis Exp 2012;(61):3892..

[106] Mei J, Hong Y, Lam JW, Qin A, Tang Y, Tang BZ. Aggregation-induced emission: the whole is more brilliant than the parts. Adv Mater 2014;26 (31):5429–79.

[107] Kumar M, Hong Y, Thorn DC, Ecroyd H, Carver JA. Monitoring early-stage protein aggregation by an aggregation-induced emission fluorogen. Anal Chem 2017;89(17):9322–9.

[108] Marzano NR et al. An α-cyanostilbene derivative for the enhanced detection and imaging of amyloid fibril aggregates. ACS Chem Neurosci 2020;11 (24):4191–202.

[109] Hong Y, Lam JWY, Tang BZ. Aggregation-induced emission: phenomenon, mechanism and applications. Chem Commun 2009;29:4332–53.

[110] Mučibabić M, Apetri MM, Canters GW, Aartsma T. The effect of fluorescent labeling on α-synuclein fibril morphology. Biochim Biophys Acta (BBA) – Proteins Proteom 2016;1864(10):1419–27.

[111] Weiss S. Fluorescence spectroscopy of single biomolecules. Science 1999;283 (5408):1676–83.

[112] Cox D et al. The small heat shock protein Hsp27 binds α-synuclein fibrils, preventing elongation and cytotoxicity. J Biol Chem 2018;293(12):4486–97.

[113] Ban T et al. Direct observation of Aβ amyloid fibril growth and inhibition. J Mol Biol 2004;344(3):757–67.

[114] Ban T, Yamaguchi K, Goto Y. Direct observation of amyloid fibril growth, propagation, and adaptation. Acc Chem Res 2006;39(9):663–70.

[115] Sackett DL, Wolff J. Nile red as a polarity-sensitive fluorescent probe of hydrophobic protein surfaces. Anal Biochem 1987;167(2):228–34.

[116] Lee JE et al. Mapping surface hydrophobicity of α-synuclein oligomers at the nanoscale. Nano Lett 2018;18(12):7494–501.

[117] Dutta AK, Kamada K, Ohta K. Spectroscopic studies of nile red in organic solvents and polymers. J Photochem Photobiol A 1996;93(1):57–64.

[118] Swain J, Mishra AK. Nile red fluorescence for quantitative monitoring of micropolarity and microviscosity of pluronic F127 in aqueous media. Photochem Photobiol Sci 2016;15(11):1400–7.

[119] Whiten DR et al. Single-molecule characterization of the interactions between extracellularchaperones and toxic α-synuclein oligomers. Cell Rep 2018;23(12):3492–500.

[120] Horrocks MH et al. Single-molecule imaging of individual amyloid protein aggregates in human biofluids. ACS Chem Neurosci 2016;7(3):399–406.

[121] Sulatskaya AI, Maskevich AA, Kuznetsova IM, Uversky VN, Turoverov KK. Fluorescence quantum yield of thioflavin T in rigid isotropic solution and incorporated into the amyloid fibrils. PloS one 2010;5(10):e15385.

[122] Pras M, Schubert M. Metachromatic properties of amyloid in solution. J Histochem Cytochem 1969;17(4):258–65.

[123] De S et al. Different soluble aggregates of Aβ42 can give rise to cellular toxicity through different mechanisms. Nat Commun 2019;10(1):1541.

[124] Sulatskaya AI, Kuznetsova IM, Turoverov KK. Interaction of thioflavin T with amyloid fibrils: fluorescence quantum yield of bound dye. J Phys Chem B 2012;116(8):2538–44.

[125] Yang F, Wilkinson M, Austin EJ, Odonnell KP. Origin of the stokes shift: a geometrical model of exciton spectra in 2D semiconductors. Phys Rev Lett 1993;70(3):323–6.

[126] Stopa B et al. The structure and protein binding of amyloid-specific dye reagents. Acta Biochim Pol 2003;50(4):1213–27.

[127] Stsiapura VI, Maskevich AA, Kuzmitsky VA, Turoverov KK, Kuznetsova IM. Computational study of Thioflavin T torsional relaxation in the excited state. J PhysChem A 2007;111(22):4829–35.

[128] Toseland CP. Fluorescent labeling and modification of proteins. J Chem Biol 2013;6(3):85–95.

[129] Wägele J, De Sio S, Voigt B, Balbach J, Ott M. How fluorescent tags modify oligomer size distributions of the Alzheimer peptide. Biophys J 2019;116 (2):227–38.

[130] Bemporad F, Chiti F. Protein misfolded oligomers: experimental approaches, mechanism of formation, and structure-toxicity relationships. Chem Biol 2012;19(3):315–27.

[131] Dresser L et al. Amyloid-β oligomerization monitored by single-molecule stepwise photobleaching. Methods 2020;193:80–95.

[132] Choi EY, Kang SS, Lee SK, Han BH. Polyphenolic biflavonoids inhibit amyloid-β fibrillation and disaggregate preformed amyloid-β fibrils. Biomol Ther (Seoul) 2020;28(2):145–51.

[133] Caruana M, Högen T, Levin J, Hillmer A, Giese A, Vassallo N. Inhibition and disaggregation of α-synuclein oligomers by natural polyphenolic compounds. FEBS Lett 2011;585(8):1113–20.

[134] Freyssin A, Page G, Fauconneau B, Rioux Bilan A. Natural polyphenols effects on protein aggregates in Alzheimer's and Parkinson's prion-like diseases. Neural Regen Res 2018;13(6):955–61.

[135] Demchenko AP. Photobleaching of organic fluorophores: quantitative characterization, mechanisms, protection. Methods Appl Fluorescence 2020;8(2).

[136] Zheng Q, Blanchard SC. Single Fluorophore Photobleaching. In: Roberts GCK, editor. Encyclopedia of Biophysics. Berlin, Heidelberg: Springer; 2013. , https://doi.org/10.1007/978-3-642-16712-6_482.

[137] Aitken CE, Marshall RA, Puglisi JD. An oxygen scavenging system for improvement of dye stability in single-molecule fluorescence experiments. Biophys J 2008;94(5):1826–35.

[138] Lakowicz JR, Weber G. Quenching of fluorescence by oxygen. A probe for structural fluctuations in macromolecules. Biochemistry 1973;12 (21):4161–70.

[139] Hines KE. Inferring subunit stoichiometry from single molecule photobleaching. J Gen Physiol 2013;141(6):737–46.

[140] Arant RJ, Ulbrich MH. Deciphering the subunit composition of multimeric proteins by counting photobleaching steps. ChemPhysChem: A Eur J Chem Phys Chem 2014;15(4):600–5.

[141] Ding H, Wong PT, Lee EL, Gafni A, Steel DG. Determination of the oligomer size of amyloidogenic protein β-amyloid(1–40) by single-molecule spectroscopy. Biophys J 2009;97(3):912–21.

[142] Johnson RD, Schauerte JA, Wisser KC, Gafni A, Steel DG. Direct observation of single amyloid-β(1–40) oligomers on live cells: binding and growth at physiological concentrations. PloS one 2011;6(8):e23970.

[143] Li J, Zhang L, Johnson-Buck A, Walter NG. Automatic classification and segmentation of single-molecule fluorescence time traces with deep learning. Nat Commun 2020;11(1):5833.

[144] Dey S, Das A, Maiti S. Correction of systematic bias in single molecule photobleaching measurements. Biophys J 2020;118(5):1101–8.

[145] Dey S, Das A, Dey A, Maiti S. Membrane affinity of individual toxic protein oligomers determined at the single-molecule level. Phys Chem Chem Phys 2020;22(26):14613–20.

[146] Orte A, Birkett NR, Clarke RW, Devlin GL, Dobson CM, Klenerman D. Direct characterization of amyloidogenic oligomers by single-molecule fluorescence. ProcNatl Acad Sci USA 2008;105(38):14424–9.

[147] Orte A, Clarke R, Balasubramanian S, Klenerman D. Determination of the fraction and stoichiometry of femtomolar levels of biomolecular complexes in an excess of monomer using single-molecule, two-color coincidence detection. Anal Chem 2006;78(22):7707–15.

[148] Narayan P et al. The extracellular chaperone clusterin sequesters oligomeric forms of the amyloid-β1−40 peptide. Nat Struct Mol Biol 2012;19(1):79–83.

[149] Sánchez L et al. Aβ40 and Aβ42 amyloid fibrils exhibit distinct molecular recycling properties. J Am Chem Soc 2011;133(17):6505–8.

[150] Grüning CSR et al. The off-rate of monomers dissociating from amyloid-β protofibrils. J Biol Chem 2013;288(52):37104–11.

[151] Zhang H, Guo P. Single molecule photobleaching (SMPB) technology for counting of RNA, DNA, protein and other molecules in nanoparticles and biological complexes by TIRF instrumentation. Methods 2014;67(2):169–76.

[152] Sherman E et al. Using fluorescence correlation spectroscopy to study conformational changes in denatured proteins. Biophys J 2008;94 (12):4819–27.

[153] Medina MA, Schwille P. Fluorescence correlation spectroscopy for the detection and study of single molecules in biology. BioEssays 2002;24 (8):758–64.

[154] Sahoo B, Drombosky K, Wetzel R. Fluorescence Correlation Spectroscopy: A tool to study protein oligomerization and aggregation in vitro and in vivo. Methods Mol Biol 2015;1345:67–87.

[155] Földes-Papp Z, Demel U, Tilz GP. Ultrasensitive detection and identification of fluorescent molecules by FCS: Impact for immunobiology. Proc Natl Acad Sci 2001;98(20):11509–14.

[156] Kitamura A, Kinjo M. State-of-the-art fluorescence fluctuation-based spectroscopic techniques for the study of protein aggregation. Int J Mol Sci 2018;19(4):964.

[157] Bulseco DA, Wolf DE. Fluorescence correlation spectroscopy: molecular complexing in solution and in living cells. Methods Cell Biol 2013;114:489–524.

[158] Adamczyk Z, Sadlej K, Wajnryb E, Ekiel-Jeżewska ML, Warszyński P. Hydrodynamic radii and diffusion coefficients of particle aggregates derived from the bead model. J Colloid Interface Sci 2010;347(2):192–201.

[159] Liu C-C, Liu C-C, Kanekiyo T, Xu H, Bu G. Apolipoprotein E and Alzheimer disease: risk, mechanisms and therapy. Nat Rev Neurol 2013;9(2):106–18.

[160] Li X et al. Early stages of aggregation of engineered α-synuclein monomers and oligomers in solution. Sci Rep 2019;9(1):1734.

[161] Auer S, Dobson CM, Vendruscolo M. Characterization of the nucleation barriers for protein aggregation and amyloid formation. HFSP J 2007;1 (2):137–46.

[162] Wu JW et al. Fibrillar oligomers nucleate the oligomerization of monomeric amyloid β but do not seed fibril formation. J Biol Chem 2010;285(9):6071–9.

[163] Lasagna-Reeves CA et al. Alzheimer brain-derived tau oligomers propagate pathology from endogenous tau. Sci Rep 2012;2(1):700.

[164] Illes-Toth E, Ramos MR, Cappai R, Dalton C, Smith DP. Distinct higher-order α-synuclein oligomers induce intracellular aggregation. Biochem J 2015;468 (3):485–93.

[165] Post K et al. Rapid acquisition of β-sheet structure in the prion protein prior to multimer formation. Biol Chem 1998;379(11):1307–18.

[166] Tjernberg LO et al. Amyloid β-peptide polymerization studied using fluorescence correlation spectroscopy. Chem Biol 1999;6(1):53–62.

[167] Sengupta P, Garai K, Balaji J, Periasamy N, Maiti S. Measuring size distribution in highly heterogeneous systems with fluorescence correlation spectroscopy. Biophys J 2003;84(3):1977–84.

[168] Nath S, Meuvis J, Hendrix J, Carl SA, Engelborghs Y. Early aggregation steps in alpha-synuclein as measured by FCS and FRET: evidence for a contagious conformational change. Biophys J 2010;98(7):1302–11.

[169] Mittag JJ, Jacobs MR, McManus JJ. Fluorescence correlation spectroscopy for particle sizing in highly concentrated protein solutions. Methods Mol Biol 2019;2039:157–71.

[170] Novo M, Freire S, Al-Soufi W. Critical aggregation concentration for the formation of early Amyloid-β (1–42) oligomers. Sci Rep 2018;8(1):1783.

[171] Kapanidis AN, Laurence TA, Lee NK, Margeat E, Kong X, Weiss S. Alternating-laser excitation of single molecules. Acc Chem Res 2005;38(7):523–33.

[172] Kapanidis AN, Lee NK, Laurence TA, Doose S, Margeat E, Weiss S. Fluorescence-aided molecule sorting: analysis of structure and interactions by alternating-laser excitation of single molecules. Proc Natl Acad Sci 2004;101(24):8936.

[173] Gao X, Gao P, Prunsche B, Nienhaus K, Nienhaus GU. Pulsed interleaved excitation-based line-scanning spatial correlation spectroscopy (PIE-lsSCS). Sci Rep 2018;8(1):16722.

[174] Müller BK, Zaychikov E, Bräuchle C, Lamb DC. Pulsed Interleaved Excitation. Biophys J 2005;89(5):3508–22.

[175] Paredes JM et al. Early amyloidogenic oligomerization studied through fluorescence lifetime correlation spectroscopy. Int J Mol Sci 2012;13 (8):9400–18.

[176] Förster T. Energy migration and fluorescence. 1946. J Biomed Opt 2012;17 (1):. https://doi.org/10.1117/1.JBO.17.1.011002011002.

[177] Bajar BT, Wang ES, Zhang S, Lin MZ, Chu J. A guide to fluorescent protein FRET pairs. Sensors 2016;16(9):1488.

[178] Miyawaki A. Development of probes for cellular functions using fluorescent proteins and fluorescence resonance energy transfer. Annu Rev Biochem 2011;80:357–73.

[179] Okamoto K, Sako Y. Recent advances in FRET for the study of protein interactions and dynamics. Curr Opin Struct Biol 2017;46:16–23.

[180] Hellenkamp B et al. Precision and accuracy of single-molecule FRET measurements—a multi-laboratory benchmark study. Nat Methods 2018;15 (9):669–76.

[181] Choi UB, Weninger KR, Bowen ME. Immobilization of proteins for single-molecule fluorescence resonance energy transfer measurements of conformation and dynamics. Methods Mol Biol 2012;896:3–20.

[182] Schmid S, Hugel T. Efficient use of single molecule time traces to resolve kinetic rates, models and uncertainties. J Chem Phys 2017;148(12):123312.

[183] Tan YW, Hanson JA, Chu JW, Yang H. Confocal single-molecule FRET for protein conformational dynamics. Methods Mol Biol 2014;1084:51–62.

[184] Okamoto K, Hiroshima M, Sako Y. Single-molecule fluorescence-based analysis of protein conformation, interaction, and oligomerization in cellular systems. Biophys Rev 2018;10(2):317–26.

[185] Li J, Uversky VN, Fink AL. Effect of familial Parkinson's disease point mutations A30P and A53T on the structural properties, aggregation, and fibrillation of human α-synuclein. Biochemistry 2001;40(38):11604–13.

[186] Zhang C et al. Amyloid-like aggregates of the yeast prion protein ure2 enter vertebrate cells by specific endocytotic pathways and induce apoptosis. PloS ONE 2010;5(9):e12529.

[187] Kim D-H et al. Direct visualization of single-molecule membrane protein interactions in living cells. PLoS Biol 2018;16(12):e2006660.

[188] Perera T, Gunasekara H, Hu YS. Single-molecule interaction microscopy reveals antibody binding kinetics. bioRxiv 2020. https://doi.org/10.1101/2020.09.21.306605.

[189] Kaur G, Lewis JS, van Oijen AM. Shining a spotlight on DNA:single-molecule methods to visualise DNA. Molecules 2019;24(3):491.

[190] Johnston CL, Marzano NR, van Oijen AM, Ecroyd H. Using single-molecule approaches to understand the molecular mechanisms of heat-shock protein chaperone function. J Mol Biol 2018;430(22):4525–46.

[191] Mashaghi A, Kramer G, Lamb DC, Mayer MP, Tans SJ. Chaperone action at the single-molecule level. Chem Rev 2014;114(1):660–76.

[192] Outeiro TF et al. Small heat shock proteins protect against α-synuclein-induced toxicity and aggregation. Biochem Biophys Res Commun 2006;351 (3):631–8.

[193] Spillantini MG, Schmidt ML, Lee VMY, Trojanowski JQ, Jakes R, Goedert M. α-Synuclein in Lewy bodies. Nature 1997;388(6645):839–40.

[194] Muchowski PJ, Wacker JL. Modulation of neurodegeneration by molecular chaperones. Nat Rev Neurosci 2005;6(1):11–22.

[195] Auluck PK, Chan HY, Trojanowski JQ, Lee VM, Bonini NM. Chaperone suppression of alpha-synuclein toxicity in a Drosophila model for Parkinson's disease. Science 2002;295(5556):865–8.

[196] Watanabe M, Dykes-Hoberg M, Culotta VC, Price DL, Wong PC, Rothstein JD. Histological evidence of protein aggregation in mutant SOD1 transgenic mice and in amyotrophic lateral sclerosis neural tissues. Neurobiol Dis 2001;8(6):933–41.

[197] Kundel F et al. Hsp70 inhibits the nucleation and elongation of Tau and sequesters Tau aggregates with high affinity. ACS Chem Biol 2018;13(3):636–46.

[198] Giese KC, Vierling E. Changes in oligomerization are essential for the chaperone activity of a small heat shock protein in vivo and in vitro. J Biol Chem 2002;277(48):46310–8.

[199] Haslbeck M, Weinkauf S, Buchner J. Small heat shock proteins: Simplicity meets complexity. J Biol Chem 2019;294(6):2121–32.

[200] Zhang K et al. A novel mechanism for small heat shock proteins to function as molecular chaperones. Sci Rep 2015;5(1):8811.

[201] Johnston CL et al. Single-molecule fluorescence-based approach reveals novel mechanistic insights into human small heat shock protein chaperone function. J Biol Chem 2021;296.

[202] Yerbury JJ et al. The extracellular chaperone clusterin influences amyloid formation and toxicity by interacting with prefibrillar structures. FASEB J 2007;21(10):2312–22.

[203] Namba Y, Tomonaga M, Kawasaki H, Otomo E, Ikeda K. Apolipoprotein E immunoreactivity in cerebral amyloid deposits and neurofibrillary tangles in Alzheimer's disease and kuru plaque amyloid in Creutzfeldt-Jakob disease. Brain Res 1991;541(1):163–6.

[204] Ellis RJ et al. Cerebral amyloid angiopathy in the brains of patients with Alzheimer's disease: the CERAD experience, Part XV. Neurology 1996;46(6):1592–6.

[205] Chartier-Harlin MC et al. Apolipoprotein E epsilon 4 allele as a major risk factor for sporadic early and late-onset forms of Alzheimer's disease: analysis of the 19q13.2 chromosomal region. Hum Mol Genet 1994;3(4):569–74.

[206] Ly S et al. Binding of Apolipoprotein E inhibits the oligomer growth of amyloid-β peptide in solution as determined by fluorescence cross-correlation spectroscopy. J Biol Chem 2013;288(17):11628–35.

[207] Garai K, Verghese PB, Baban B, Holtzman DM, Frieden C. The binding of apolipoprotein E to oligomers and fibrils of amyloid-β alters the kinetics of amyloid aggregation. Biochemistry 2014;53(40):6323–31.

[208] Jäkel L, Biemans EALM, Klijn CJM, Kuiperij HB, Verbeek MM. Reduced influence of apoE on Aβ43 aggregation and reduced vascular Aβ43 toxicity as compared with Aβ40 and Aβ42. Mol Neurobiol 2020;57(4):2131–41.

[209] Duennwald ML, Echeverria A, Shorter J. Small heat shock proteins potentiate amyloid dissolution by protein disaggregases from yeast and humans. PLoS Biol 2012;10(6):e1001346.

[210] Gao X et al. Human Hsp70 disaggregase reverses Parkinson's-linked α-synuclein amyloid fibrils. Mol Cell 2015;59(5):781–93.

[211] De Los Rios P, Ben-Zvi A, Slutsky O, Azem A, Goloubinoff P. Hsp70 chaperones accelerate protein translocation and the unfolding of stable protein aggregates by entropic pulling. Proc Natl Acad Sci USAa 2006;103(16):6166–71.

[212] Sousa R, Lafer EM. The physics of entropic pulling: a novel model for the Hsp70 motor mechanism. Int J Mol Sci 2019;20(9):2334.

[213] Lee S, Lee J, Hohng S. Single-molecule three-color FRET with both negligible spectral overlap and long observation time. PLoS ONE 2010;5(8):e12270.

[214] Yoo J, Kim J-Y, Louis JM, Gopich IV, Chung HS. Fast three-color single-molecule FRET using statistical inference. Nat Commun 2020;11(1):3336.